Studying Soil Undrained Shear strength Due to Driving Piles Using Seismic Cross-Hole Technique

Dr. Hussein H. Karim
Building and Construction Engineering Department, University of Technology/ Baghdad
Email:husn_irq@yahoo.com
Dr. Mahmoud R. AL-Qaissy
Building and Construction Engineering Department, University of Technology/Baghdad
Wisam Rahi Hasan
Building and Construction Engineering Department, University of Technology/ Baghdad

Received on:26/1/2014 & Accepted on:13/5/2014

ABSTRACT

The study is intended for geotechnical engineers who deal with the construction of deep foundations using driving piles with the implementation of seismic cross-hole technique to estimate the accompanying increase (or decrease) in soil shear strength. The study concluded that there is a direct relation between the increases in soil undrained shear strength with yield stress ratio and reverse relation with moisture water content and void ratio. The increase in undrained shear strength is observed in the clay soil layer at 3-5 m in depth with low moisture content and void ratio due to the effect of time. While at depth of 1-3 m, the reverse was noticed, this decrease is attributed to the upward displacement of the soil due to shear force from driven pile and then leading to increase the soil moisture content and void ratio. The study also concluded that an increase in undrained shear strength and yield stress ratio causing a decrease in void ratio and moisture content due to the effect of aging factor. The present results have provided good overall views of the shear strength increases and their distributions and the estimated values are also of the right sizes.

Keywords: Driving pile, Seismic cross-hole, Soil shear strength, Soil aging

دراسة مقاومة القص غيرالمبزول للتربة نتيجة ركائز الدق باستخدام تقنية الابار المتقاطعة الزلزالية

الخلاصة

ان هذه الدراسة موجهة الى مهندسي الجيوتكنيك الذين يتعاملون مع انشاء الأساسات العميقة باستخدام ركائز الدق من خلال تنفيذ تقنية الابار المتقاطعة الزلزالية لتقدير الزيادة (أو النقصان) المصاحبة لمقاومة قص التربة. خلصت الدراسة الى ان هنالك علاقة طردية بين زيادات مقاومة القص غيرالمبزول للتربة مع

https://doi.org/10.30684/etj.32.10A.8
2412-0758/University of Technology-Iraq, Baghdad, Iraq

نسبة إجهاد الخضوع وعكسية مع محتوى ماء الرطوبة و نسبة الفراغات. لوحظت زيادة مقاومة القص غيرالمبزول في طبقة التربة الطينية في العمق 3-5 متر مع انخفاض محتوى الرطوبة و نسبة الفراغات بسبب تأثير الزمن. بينما في العمق 1-3 م، لوحظ العكس ويعزى هذا النقصان الى ازاحة التربة للاعلى بسبب قوى القص الناتجة من طرق الركيزة و والتي أدت الى زيادة المحتوى المائي ونسبة الفراغات في التربة. كما خلصت الدراسة إلى أنه أي زيادة في مقاومة القص غيرالمبزول ونسبة إجهاد الخضوع تسبب انخفاض في نسبة الفراغات ومحتوى الرطوبة بسبب تأثيرعامل العمر. وفرت النتائج الحالية نظرة جيدة عموما في زيادات مقاومة القص وتوزيعاتها والقيم المقدرة لها بنسب معقولة.

INTRODUCTION

There is an increasing application of seismic parameters for geotechnical determination for various underground constructions. Two demands arise in utilizing the correlation between seismic data and geotechnical properties; the first is to improve the measuring procedure and to refine the interpretation techniques; and the second is to increase the understanding of the significance of seismic parameters for geotechnical determinations [1, 2, 3].

Correlations between seismic velocities and other geotechnical properties (such as moisture content *M.C,* liquid limit *L.L,* plasticity index *P.I,* saturated unit weight γ_{sat}, compression index C_c, swelling index C_r, void ratio *e,* effective confining pressure σ_P, effective overburden pressure σ_v', unconfined compression strength q_c, ultimate bearing capacity q_u and standard penetration number N, preconsolidation pressure P_c, Poisson's ratio μ and lateral earth pressure coefficient at rest K_o cohesion C and the angle of friction ϕ) have been studied, based upon velocity data for different geographical sites. These correlations could be used to give rather accurate predictions on the geotechnical properties for construction purposes. By comparing the different properties, indications may be obtained where the optimum soil/rock conditions for a certain site are to be encountered [1, 2, 3, 4, 5].

Such applications are intended for geotechnical engineers who deal with the construction of deep foundation using driving pile, who design and carry out field investigations and who develop methods for prediction of consolidation processes resulting in significant setup pile capacity and shear increases. For instance, the method of seismic cross-hole has the advantage of not requiring access to the driving piles itself and provides a continuous mapping of the properties in the entire soil volume in the investigated section, not only in selected test points [6].

The present work deals with a new method for assessing undrained shear strength associated with driving piles using seismic cross-hole technique. In addition, stress relaxation (creep) in the surrounding soil arch and soil aging will be studied.

Theoretical Background

Very limited data are available documenting the interaction between the seismic wave velocities and the soil during ground improvement by pile driving. Seismic waves measurement and numerical analysis are used to provide insights into the physical process of ground improvement.

The fundamental relationships between the velocity of the wave propagation and the physical properties of the materials through which the waves pass are independent of the

frequency of the waves. Body waves are non-dispersive; that is, all frequency components in a wave train or pulse travel through any material at the same velocity, determined only by the elastic modulus and density of the material. One application of shear wave seismology is in engineering site investigation where the separate measurement of compressional wave V_P and shear wave V_S for near-surface layers allows direct calculation of Poisson's ratio and estimation of the elastic moduli, which provide valuable information on the in situ geotechnical properties of the ground [7].

The measurement of in situ stresses has proved very difficult due to soil-structure interaction. Seismic wave velocity measurement may be employed in the in situ (field) techniques such as cross-hole method, which is much less influenced by the details at the soil-structure interface and it can be used to estimate in situ stress. Since relationships between the velocity and stress are well established. Seismic data may be also used to estimate in situ stresses during pressed-in piling and to explore a cavity expansion view of the pile base capacity mobilization mechanism following the success of spherical cavity expansion solutions in predicting this measured stress field [8].

When a pile is driven within the soil, there is an extensive remolding of the surrounding soil and an immediate increase in the pore pressure in the soil vicinity of the pile. This phenomenon is referred to as pile "setup". The consolidation of the surrounding soil after the pile is driven plays a dominant role in the setup process. As the consolidation progresses, the horizontal (or radial) effective stress in the soil at the interface between the soil and the pile increases. This increase in the effective stress leads to an increase in the maximum frictional resistance offered by the soil to the pile, which results an increase of pullout resistance [9, 10].

It has been shown that there is a direct relation between soil preconsolidation pressure and undrained shear strength as stated by Ladd and Foott (1974) [11]. This relation is valid independent on whether the preconsolidation pressure has been created directly by an acting effective stress or as indirect by creep effects.

Moreover, seismic cross-hole tomography has been tried to estimate the increase in shear strength due to consolidation below the embankments [6]. This study is considered to be a pilot project in order to assess if the method can be used in practical applications and to what accuracy the shear strength increase can be estimated.

Study Area

The present study was carried out at Al-Hur waste water treatment plant project (Al-Hur city 15 km west Karbala Governorate) to study the effect of driven pile (soil/pile setup) on soil properties with the assistance of seismic cross-hole technique. Some geotechnical properties were obtained from field measurements using seismic cross-hole technique. The layout of site plan with the location of boreholes is shown in Figure 1.

Field Work, Samples Recovery and Testing Methods

The field work in the site includes three main stages: the subsurface exploration represented by field borings and samples recovery, seismic cross-hole surveying and pile driving.

Stage I- Subsurface Exploration

Field Borings and Samples Recovery

To execute the required activities of this investigation, 5 bore holes of 15 m depth were drilled in the site by National Center for Construction Labs and Research. These boreholes are described as follows:

a. Two boreholes were drilled inside and outside the group pile. One of them for sampling and performed standard penetration tests (S.P.T). The location of these boreholes is shown in Figure 2. These boreholes were cased by plastic pipe (PVC) of 75 mm in diameters to resist lateral pressure. The clear space between the pipe edges and borehole wall was filled by a granular soil material to make firm contact between the plastic pipe and the borehole shaft. Also, these boreholes were used to receive the seismic waves in cross-hole survey.

b. Another three boreholes were drilled outside the pile group as sources to generate seismic compression (P) and shear (S) waves in seismic cross-hole survey. The source of seismic waves is denoted as S in Figure 1 before and after driven pile.

Samples Recovery

Representative samples were taken along the borehole with depth interval ranging between 1.5-3.0 m and when the strata change. The undisturbed samples (UD) were taken by Shelby tubes from 2 m and 4 m in depth. The disturbed samples (DS) were taken by auger at different depths. The split spoon samples (SS) were obtained from standard splits spoon utilized in standard penetration test (S.P.T).

In Situ and Laboratory Tests

In situ standard penetration tests were conducted at various depths in the field especially in cohesionless layer. These values should be corrected according to the G.W.T and overburden pressure as shown in borehole log (Fig. 2).

Disturbed samples taken from boreholes were used for soil classification and chemical tests. All tests were carried out according to the recommendation and procedures described by ASTM and B.S standards as appropriate or applicable for any given case. The laboratory test results are summarized in Table 1.

Stage II- Seismic Cross-hole Surveying: ABEM Terraloc Mark II seismic system is used to record all of the seismic cross-hole waves, it has a high ability of analysis of seismic recording to shallow depth. The ABEM Terraloc consists of two main separate units as shown in Figure 3 a and b. The field information units consist of printer unit and boreholes pickup model 3315 which are seismic receivers designed to measure P and S wave velocity in borehole consisting three geophones, two horizontal and one vertical. Vertical shear and compressional waves propagating in a horizontal layer were detected by two receivers placed in adjacent boreholes at the same depth as the energy source (Fig. 4). The results were printed on seismic record using Terraloc ABEM. The data of Vertical Seismic Profile (VSP) are monitored and displayed as seismograms. The final process represents picking the first of P-waves and second arrivals of S-waves for each trace.

Stage III- Pile driving: After measuring seismic cross-hole in the site of Al-hur project, 60 precast concrete piles of 285 mm ***** 285 mm cross section area were driven on construction biological tank at spacing 2.18 m in X-direction and 2.93 m in Y-direction.

Results and Discussion

Seismic Cross-Hole Technique

The measurements have been made with readily available commercial equipment and the evaluation of the compression and shear waves arrival has been made. Owing mainly to the source of the seismic waves, the installation of the measuring equipment was relatively laborious, costly and time demanding. The tests were also performed in homogeneous soil profiles in which the picking of arrival times of both compression wave (V_P) and shear wave (V_S) for each depth was straightforward and did not require any filtering of the signals. Thus the first arrivals have been calculated directly from the records. The geometries of the measured sections were also favorable for this type of measurement.

Seismic Velocities Versus Depth

The velocities of compression wave (V_P) and shear wave (V_S) for each depth have been calculated. The relationship between compression and shear wave velocities with depth for each profile are shown in Figures 5 and 6.

Examining seismic velocities for both Vertical Seismic Profile (VSP) and for both V_P and V_S presented in above figures, it is obvious that both velocities increase with depth with a noticeable increase at the depth 7-9 m.

For seismic profile S1 before driven piles, an increase in both V_P and V_S velocities particularly at depth ($\geqslant$8m). The average values of V_P and V_S for depth 0-8 m are 720 and 192 m/sec respectively. While for depth (8-15 m), the average values of V_P and V_S are 2034 and 551 m/sec respectively. Thus, it is clear that the increase in both velocities is about 3 times for the depths more than 8 m.

The increase or decrease in both seismic velocities is attributed to aging phenomena. Aging occurs when seismic wave velocities increase with time and lead to increase pile capacity (soil/pile setup). The creep effect is clearly appeared at depth 3-5 m due to secondary consolidation. In addition, the increase or decrease in seismic velocity reflects the soil due to pile driving which is indicated by the increase of void ratio at depth 1-3 m and decrease at 4-5 m.

Shear Strength after Complete Pore Water Pressure

1. Relation of shear strength with void ratio

The relationship of V_P and void ratio is illustrated in an empirical equation [1]:

$$e = \frac{1}{\left(-2.489+\left(0.63\ ln(V_P)\right)\right)} \quad \ldots(1)$$

In a similar way, the relation of V_S with void ratio is shown in equation below [1]:

$$e = 0.582\ V_S^{(13.1/V_S)} \quad \ldots(2)$$

The correlation between shear wave velocity and void ratio using Eq. (2) is shown in Figure 7 for clay layer.

Soil that has been subjected to aging, thixotropic hardening and/or cementation will have a greater strength and stiffness in its intact state than the same soil with breakdown of the micro-structure. As the soil consolidates under the increasing overburden weight, the vertical effective stress, σ'_v, increases and the void ratio, e, decreases along a characteristic line "Sedimentation Compression Line" (SCL). This soil is said to be "normally consolidated", since the consolidation pressure (σ'_v) is the largest effective stress that the young soil has been subjected to. While the soil remains normally consolidated, the vertical yield stress, σ'_{vy} (which is commonly referred to as the preconsolidation pressure, or maximum past pressure, and denoted by σ'_p), remains equivalent to σ'_v, and σ'_{vy} increases along the SCL as the void ratio decreases during primary consolidation. Once the deposition of overburden is complete, and any excess pore pressure has dissipated, the e-σ'_v state of the soil will have reached point I on Figure 8, at which point the vertical effective stress will be σ'_{vo}, and the vertical yield stress will be (σ'_{vy})I.

Under constant effective stress, fine-grained soils continued to experience a decrease in volume due to secondary consolidation (indicated as $\Delta e_s(t)$ on Figure 8). It has been observed that σ'_{vy} continues to increase during this aging period, while the vertical effective stress remains constant at σ'_{vo}. To explain this observed increase in yield stress with time, Bjerrum (1967) [12] proposed a conceptual model in which σ'_{vy} continues to follow the SCL as the void ratio decreases with time. The resulting increase in the yield stress ratio, YSR = $\sigma'_{vy}/\sigma'_{vo}$ (which is more commonly referred to as the overconsolidation ratio, denoted by OCR), has the same net effect as if the soil had been preconsolidated to σ'_{vy} and then unloaded. Since the soil has not actually been subjected to any historical unloading, this form of aging-induced overconsolidation is sometimes referred to as "quasi-preconsolidation". After sufficient time has passed, the yield stress will reach point A on the SCL on Figure 8, and $YSR_A = (\sigma'_{vy})_A/\sigma'_{vo}$. Between points I and A, the peak undrained shear strength, S_u, of the soil tends to increase as σ'_{vy} increases, according to the S_u/σ'_{vy} ratio of the soil, which remains essentially constant during primary consolidation and aging.

Once the rate of decrease in void ratio becomes slow enough, thus thixotropic bonding of the soil particles can occur. This thixotropic hardening causes an additional increase in vertical yield stress $\bar{\sigma}_{vy}$ that is independent of void ratio, thereby causing $\bar{\sigma}_{vy}$ to displace to the right of the Sedimentation Compression Line SCL, which serves to further increase the yield stress ratio, YSR of the soil. Where YSR = is the ratio of vertical yield stress to overburden pressure $\bar{\sigma}_{vy}/\bar{\sigma}_{vo}$ (which is more commonly referred to as the over consolidation ratio, OCR). This process is illustrated in Figure 8 by the dashed segment between points A and P. It should be noted that cementation at the particle contacts will have a similar effect on $\bar{\sigma}_{vy}$ as thixotropic hardening. Between points A and P, S_u continues to increase as $\bar{\sigma}_{vy}$ increases, although the $S_u/\bar{\sigma}_{vy}$ ratio of the soil may be altered.

Thus, for a natural soil with an in-situ e_o and σ'_{vo} (point O on Figure 8), the yield stress would be $(\sigma'_{vy})_P$ and the peak undrained shear strength would be $(S_u)_o$. A typical

stress-strain curve for such a structured soil during undrained shearing is shown in the inset of Figure 8. The prefailure shearing response tends to be relatively stiff and failure tends to be brittle, with a dramatic post-peak drop in strength, due to the shear-induced destruction of the inter-particle bonds and the resulting collapse of the soil structure.
For a soil that has been destructured under undrained conditions, the void ratio will decrease during reconsolidation as the effective stress ($\bar{\sigma}$) increases, according to the slope of the destructured compression line (DCL) as stated by Weech (2002) [13] and illustrated conceptually in Figure 9. Once excess pore pressure dissipation is complete (end of primary consolidation – EOP), the effective stress will be at $\bar{\sigma}_c$ and the soil will have a void ratio of e_{EOP}. If the soil was normally consolidated before pile installation, or if the soil was completely destructured during pile installation, the yield stress at the end of reconsolidation, $\bar{\sigma}_y$(EOP), will be equivalent to $\bar{\sigma}_c$.

During aging, the void ratio (e) decreases with time at constant $\bar{\sigma}$ due to the secondary compression of the new soil fabric, as illustrated in Figure 9 [13]. The decrease in void ratio due to secondary compression, $\Delta e_s(t)$, is typically calculated using the following expression [13]:

$$\Delta e_s(t) = C_\alpha . \log(t/t_{EOP}) \quad \ldots(3)$$

where C_α= coefficient of secondary compression, and t, t_{EOP} = time since pile installation and time to end of primary consolidation (i.e. full pore pressure dissipation), respectively.

As the void ratio decreases during aging, the yield stress will tend to increase along the governing e-log$\bar{\sigma}$ compression line of the soil. Bjerrum (1967) [12] described this effect as an apparent increase in preconsolidation pressure. This is illustrated in Figure 9 for a soil that has been completely destructured, such that $\bar{\sigma}_y$ (EOP) = $\bar{\sigma}_c$. Accordingly, the relative increase in yield stress depends on the slope of the e-log$\bar{\sigma}$ compression line (which is typically referred to as the compression index, C_c) according to the following expression [13]:

$$\log[\bar{\sigma}_y(t)/\bar{\sigma}_y(EOP)] = \Delta e_s(t)/C_c \quad \ldots (4)$$

where $\bar{\sigma}_y(EOP)$ and $\bar{\sigma}_y(t)$ are the yield stresses at the end of the pore pressure dissipation period and after aging to time t, respectively. Since the ratio of $S_u/\bar{\sigma}_y$ is essentially constant for a given soil, the relative increase in shear strength should be equivalent to the relative increase in yield stress and can therefore be expressed as follows [13]:

$$S_u(t)/S_u(EOP) = 10^\alpha \quad \ldots (5)$$

$$\text{where } \alpha = \Delta e_s(t)/C_c \quad \ldots (6)$$

where $S_u(EOP)$ and $S_u(t)$ are the undrained shear strengths at the end of the pore pressure dissipation period and after aging to time t where t, t_{EOP} in this study is 6 and 1

month respectively. The results of correlation between undrained shear strength with void ratio and yield stress are illustrated in Table 2, while the results of the percent increase (or decrease) in undrained shear strength with void ratio are illustrated in Table 3. The increase in shear strength with decreasing void ratio is attributed to creep.

Relation of shear strength with moisture content

It is important to note that $M.C$ affects the value of density which brings about a corresponding change in velocity. On other hand an excess of $M.C$ means increasing voids filled with water which give a lower value of V_P. Thus an inverse relationship between V_P and $M.C$ has been expressed in an empirical equation [1]:

$$M.C = \frac{15.38\, V_P}{(V_P - 150.6)} \quad \ldots(7)$$

Similarly, the same behavior is recorded for V_S against $M.C$ but with lower values for V_S (around a half of V_P values) as shown in the following empirical relation [1]:

$$M.C = \frac{1}{\left(-0.093 + 0.0253\, ln(V_S)\right)} \quad \ldots(8)$$

The correlation between shear wave velocity and moisture content using Eq. (8) is presented as the variation of moisture content with depth for profiles S1 and S2 (Fig. 10). There are several ways in which the state and yield stress ratio (YSR) of a natural soil can change and some involve changes of the water content. If soil is left under a constant effective stress there will be continued deformations which are due to creep. In soils, creep is greatest in fine grained (clay) soils. The effects of creep in fine-grained soil (Fig. 11a) are similar to those due to compression by vibration of coarse grained (sand) soil except vibration compression occurs more or less instantaneously while creep occurs slowly and at a rate which diminishes with time. During vibration or creep compression only the water content of soil changes [14]. Examining profile S1, the moisture content decreases at two depth intervals (from 3 to 8 m and from 12 to15 m). While for profile S2, the moisture content decreases at depths (3 to 5 m and 11 to 15 m). After installation the pile, the compression surrounded soil at constant effective stress by vibration (in sand layer) or creep (in clay layer) is shown in Figure 11a. Creep is occurred in profile S1 and S2 at depth (3-5 m). The basic constitutive equation for creep is given in the following form [14]:

$$\delta w = C_\alpha \ln(t/t_o) \quad \ldots(9)$$

And so the water content decreases with the logarithm of time, as illustrated in Figure 9b. The same effect of creep observed in Figure10. The decreases in water content for the two profiles are at depth (3-5 m). Using the same idea of Figure 7, Eq. (4) can be used to calculate the increase in undrained shear strength.

During aging, the moisture content ($M.C$) decreases with time at constant $\bar{\sigma}$ due to the secondary compression of the new soil fabric as illustrated in Figure 11 [14]. The

decrease in moisture content due to secondary compression, $\delta w\,(t)$, is typically calculated using the following expression [14]:

$$\delta w(t) = C_{\alpha}.\log(t/t_{EOP}) \quad \ldots (10)$$

As the moisture content $(M.C)$ decreases during aging, the yield stress will tend to increase along the governing δw-log$\bar{\sigma}$ as shown in Figure 11. The yield stress ratio increases because the yield stress increases from $\bar{\sigma}_{ya}$ to $\bar{\sigma}_{yb}$. For a soil that has been completely destructured, such that $\bar{\sigma}_{y}$(EOP) = $\bar{\sigma}_{ya}$. Accordingly, the relative increase in yield stress depends on the slope of the δw-log$\bar{\sigma}$ compression line (which is typically referred to as the compression index, C_c) according to the following expression:
]

$$\log[\bar{\sigma}_y(t)/\bar{\sigma}_y(EOP)] = \delta w(t)/C_c \quad \ldots(11)$$

Since the ratio of $S_u/\bar{\sigma}_y$ is essentially constant for a given soil, the relative increase in shear strength should be equivalent to the relative increase in yield stress and can therefore be expressed as follows:

$$S_u(t)/S_u(EOP) = 10^{\alpha} \quad \ldots (12)$$

where $\alpha = \delta w(t)/C_c$ …(13)

The results of correlation between undrained shear strength with moisture content and yield stress are illustrated in Table 4, while the results of the percent increase (or decrease) in undrained shear strength with moisture content are illustrated in Table 5.

From the aforementioned results, the effect of time (aging) was clearly appeared at clay layer at depth 3-5 m. Where the increase of yield stress ratio and undrained shear strength besides the decrease of moisture water content and void ratio due to pile driving. While at depth of 1-3 m, the reverse was noticed because of the upward displacement of the soil due to shear force from driven pile and then leading to increase the moisture water content and void ratio. It may be stated that there is a direct relation between the increase in undrained shear strength with yield stress ratio and reverse relation with moisture water content and void ratio. Thus, an increase in undrained shear strength and yield stress ratio leading a decrease in void ratio and moisture content due to effects of driving piles and aging factor. The study concluded that as shear strength increases, void ratio and moisture content decrease. The results have provided good overall views of the shear strength increases and their distributions and the estimated values are also of the right sizes.

Table. (1). Laboratory test results.

MINISTRY OF CONSTRUCTION & HOUSING
NATIONAL CENTER FOR CONSTRUCTION LABS &

PROJECT: Waste Water Treatment Plant
At Al- Hur / Sacred Karbala

Borehole No.: 1

RECORD OF TEST RESULTS

Samples		Type	Depth of Sample		Index Property				Particle Size Distribution & Hydrometer				S.P.T. "N" Val.	Symbol	Description of Soil	Chemical Tests					
Field No.	Lab No.		From (m)	To (m)	M.C. %	L.L. %	P.I. %	L.Sh. %	Clay %	Silt %	Sand %	Grav el %				so_3 %	Gyp %	$CaCO_3$ %	TSS %	Org %	pH	Cl %
1	12793	D	0.0	1.0					24	33	24	19	—	CL	Brown lean clay with gravel .	0.83				0.37		0.83
2	12794	U	1.0	1.5	28	41	18	10	32	54	14	0	—	CL	Brown lean clay .	0.87						
3	12795	SS	1.5	2.0		60	35						9	CL	Stiff brown to green lean clay .	0.91	1.68	43			9.28	
4	12796	U	3.0	3.5	31	77	50						—	CL	Brown lean clay .							
5	12797	SS	3.5	4.0					44	54	2	0	15	CL	Stiff brown lean clay .	3.05						0.99
6	12798	SS	5.5	6.0						8	92	0	5	SW-SM	Loose brown to grey silty sand .	3.81	7.63					
7	12799	SS	7.5	8.0									20	SW-SM	Medium grey silty sand .	1.12				0.08		
8	12800	SS	9.5	10.0						1	98	1	73/6"	SW	Very dense grey silty sand .							
9	12801	SS	12.0	12.5									—	SW	Grey silty sand .	4.57	9.82				9.25	0.53
10	12802	SS	14.5	15.0						18	78	4	50/3"	SM	Very dense grey silty sand .							
11	12803	water sample														0.73					7.78	3.20
W.T =1.2 m under N.G.S.																						

Table (2). Correlation between undrianed shear strength with void ratio and yield stress.

a. Profile S1

Depth (m)	e_o before driven pile	e 1-month after driven pile	e 6-month after driven pile	$\bar{\sigma}_y$ before driven pile	$\bar{\sigma}_y$ 1-month after driven pile	$\bar{\sigma}_y$ 6-month after driven pile	S_u before driven pile	S_u 1-month after driven pile	S_u 6-month after driven pile
1	0.91	0.92	0.94	161.71	148.85	136.34	30	27.61	25.29
2	0.83	0.84	0.86	249.32	225.39	202.25	30	27.12	24.34
3	0.81	0.83	0.83	285.64	249.32	249.32	94	82.05	82.05
4	0.84	0.83	0.76	234.50	249.32	407.97	94	99.94	163.53
5	0.85	0.83	0.77	221.78	249.32	390.58	94	105.67	165.55

b. Profile S2

Depth (m)	e_o before driven pile	e 1-month after driven pile	e 6-month after driven pile	$\bar{\sigma}_y$ before driven pile	$\bar{\sigma}_y$ 1-month after driven pile	$\bar{\sigma}_y$ 6-month after driven pile	S_u before driven pile	S_u 1-month after driven pile	S_u 6-month after driven pile
1	0.9	0.94	0.99	171.57	144.12	118.25	30	25.20	20.68
2	0.87	0.865	0.91	200.51	231.76	179.93	30	34.68	26.92
3	0.83	0.79	0.83	241.87	331.67	249.32	94	128.90	96.89
4	0.84	0.79	0.8	238.18	331.67	309.38	94	130.90	122.10
5	0.79	0.78	0.77	329.62	335.77	364.96	94	95.75	104.08

Table (3). Increase (or decrease) in shear strength percentage with void ratio.

a. Profile S1

Depth (m)	e (1-month after driven pile)	e (6-month after driven pile)	C_c	S_u(1-month) /S_u (before)	$S_u(t)/S_u(EOP)$
1	0.92	0.94	0.22	-0.92	-0.81
2	0.84	0.86	0.22	-0.90	-0.81
3	0.83	0.83	0.22	-0.87	1
4	0.83	0.76	0.22	+1.06	+2
5	0.83	0.77	0.22	+1.12	+1.87

b. Profile S2

Depth (m)	e (1-month after driven pile)	e (6-month after driven pile)	C_c	S_u(1-month)/S_u (before)	$S_u(t)/S_u(EOP)$
1	0.94	0.99	0.23	-0.84	-0.67
2	0.865	0.91	0.23	+1.15	-0.74
3	0.79	0.83	0.22	+1.37	-0.73
4	0.79	0.8	0.22	+1.39	-0.9
5	0.78	0.77	0.22	+1.018	+1.11

Table (4). Correlation between undrained shear strength with moisture content and yield stress.

a. Profile S1

Depth (m)	$M.C$ before driven pile	$M.C$ 1-month after driven pile	$M.C$ 6-month after driven pile	$\bar{\sigma}$y before driven pile	$\bar{\sigma}$y 1-month after driven pile	$\bar{\sigma}$y 6-month after driven pile	S_u before driven pile	S_u 1-month after driven pile	S_u 6-month after driven pile
1	30	25	27	161.71	148.85	136.34	30	27.61	25.29
2	25	26	27	249.32	225.39	202.25	30	27.12	24.34
3	23	25	25	285.64	249.32	249.32	94	82.05	82.05
4	25	25	20	234.50	249.32	407.97	94	99.94	163.53
5	26	25	21	221.78	249.32	390.58	94	105.67	165.55

b. Profile S2

Depth (m)	$M.C$ before driven pile	$M.C$ 1-month after driven pile	$M.C$ 6-month after driven pile	$\bar{\sigma}$y before driven pile	$\bar{\sigma}$y 1-month after driven pile	$\bar{\sigma}$y 6-month after driven pile	S_u before driven pile	S_u 1-month after driven pile	S_u 6-month after driven pile
1	29	32	36	171.57	144.12	118.25	30	25.20	20.68
2	27	27	30	200.51	231.76	179.93	30	34.68	26.92
3	25	22	25	241.87	331.67	249.32	94	128.90	96.89
4	25	22	23	238.18	331.67	309.38	94	130.90	122.10
5	22	22	21	329.62	335.77	364.96	94	95.75	104.08

Table (5). Increase (or decrease) in undrained shear strength with moisture content.

a. Profile S1

Depth (m)	$M.C$ (1-month after driven pile)	$M.C$ (6-month after driven pile)	C_c	S_u(1-month) /S_u (before)	$S_u(t)/S_u(EOP)$
1	25	27	0.22	0.92	0.81
2	26	27	0.22	0.90	0.9
3	25	25	0.22	0.87	1
4	25	20	0.22	1.06	1.68
5	25	21	0.22	1.12	1.51

b. Profile S2

Depth (m)	$M.C$ (1-month after driven pile)	$M.C$ (6-month after driven pile)	C_c	S_u(1-month) /S_u (before)	$S_u(t)/S_u(EOP)$
1	32	36	0.23	0.84	0.67
2	27	30	0.23	1.15	0.74
3	22	25	0.22	1.37	0.73
4	22	23	0.22	1.39	0.9
5	22	21	0.22	1.018	1.11

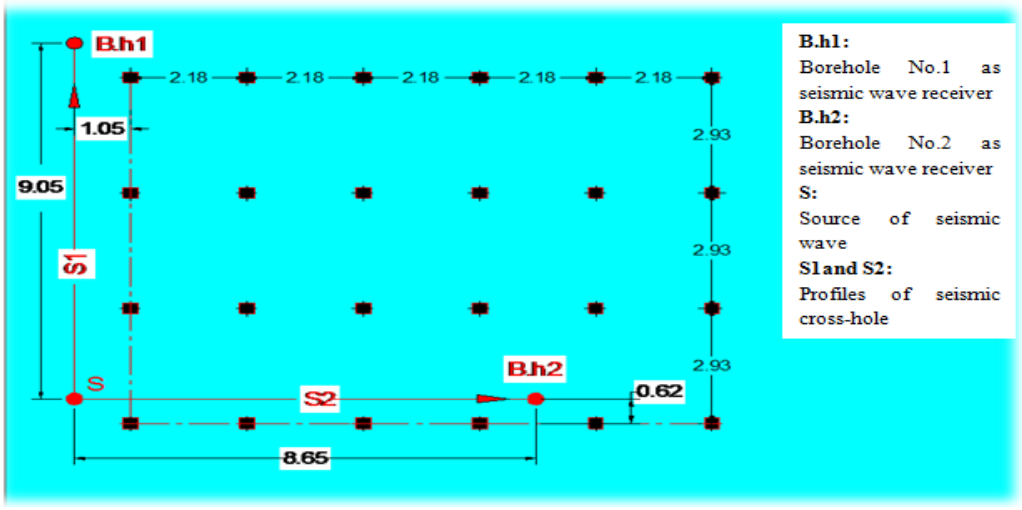

Figure (1). Site plan showing bore-holes locations.

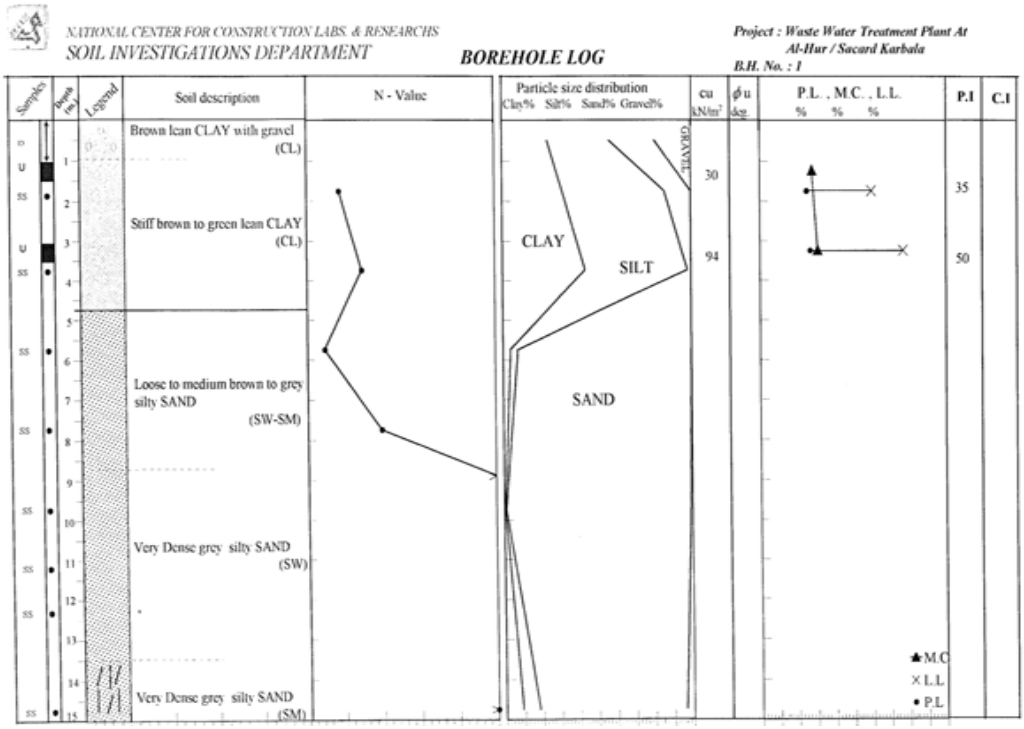

Figure (2). Borehole log No.1.

(a) (b)

Figure (3). ABEM Terraloc Mark II: (a) Seismic system and printer. (b) Boreholes pickup (Model 3315) used in the site.

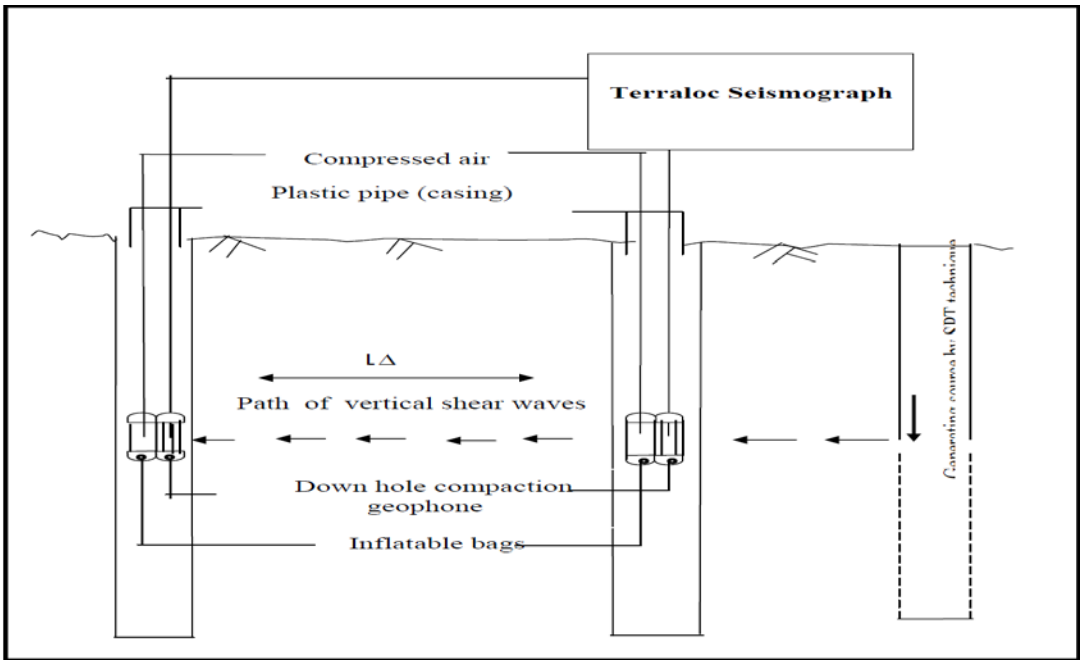

Figure (4). Seismic cross-hole technique.

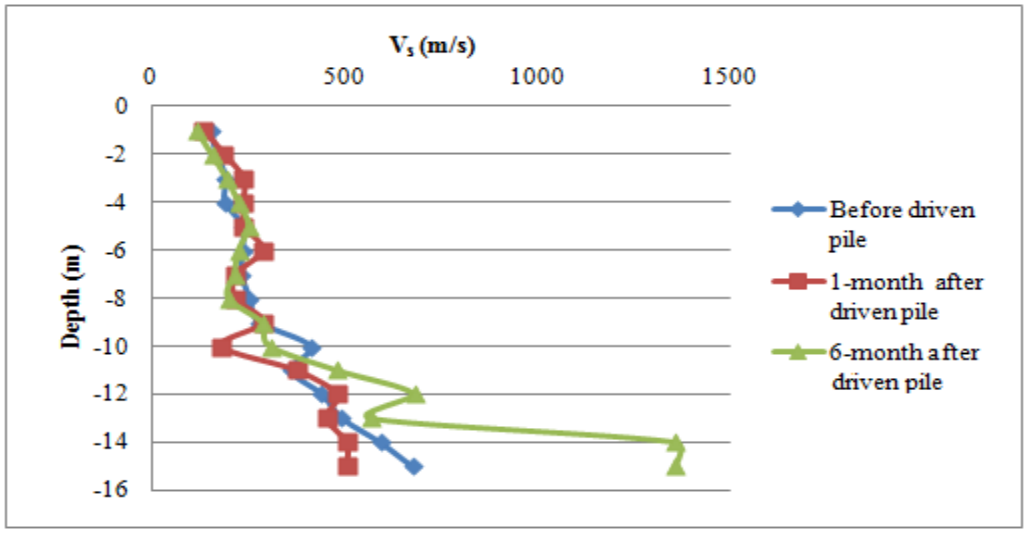

(a) Profile S1

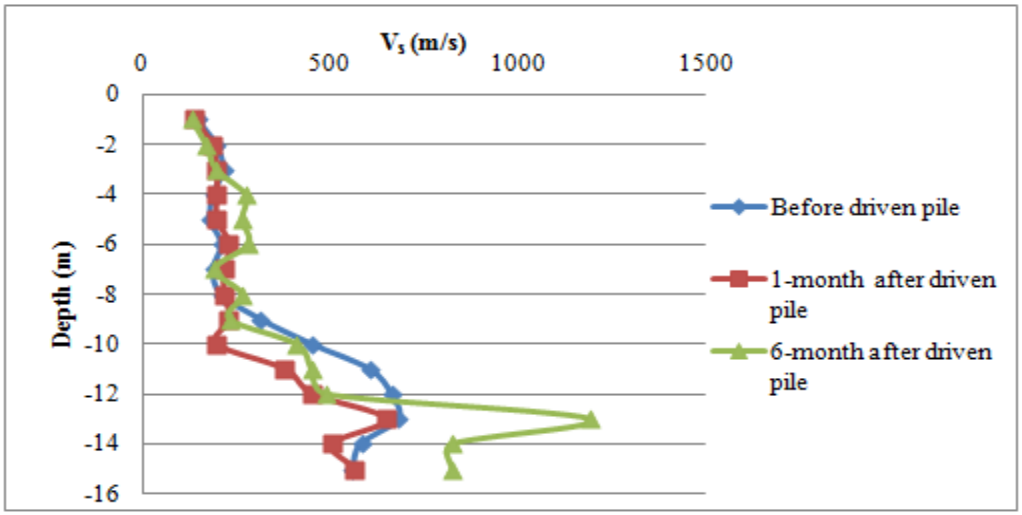

(b) Profile S2

Figure (5). Relationship between shear wave velocity versus depth for Profiles S1 and S2 before driven piles and after (1-6) month.

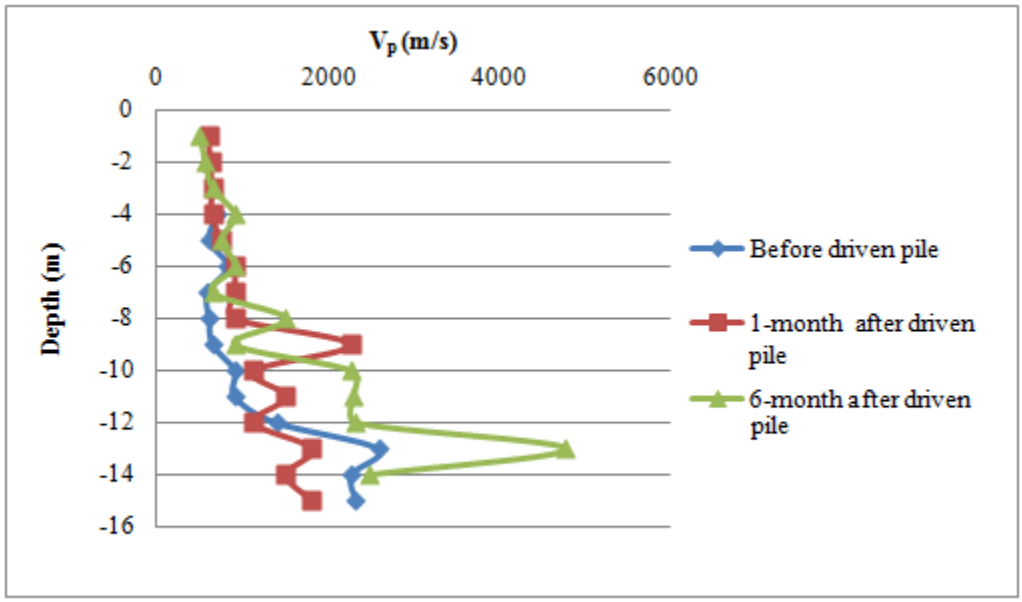

(a) Profile S1

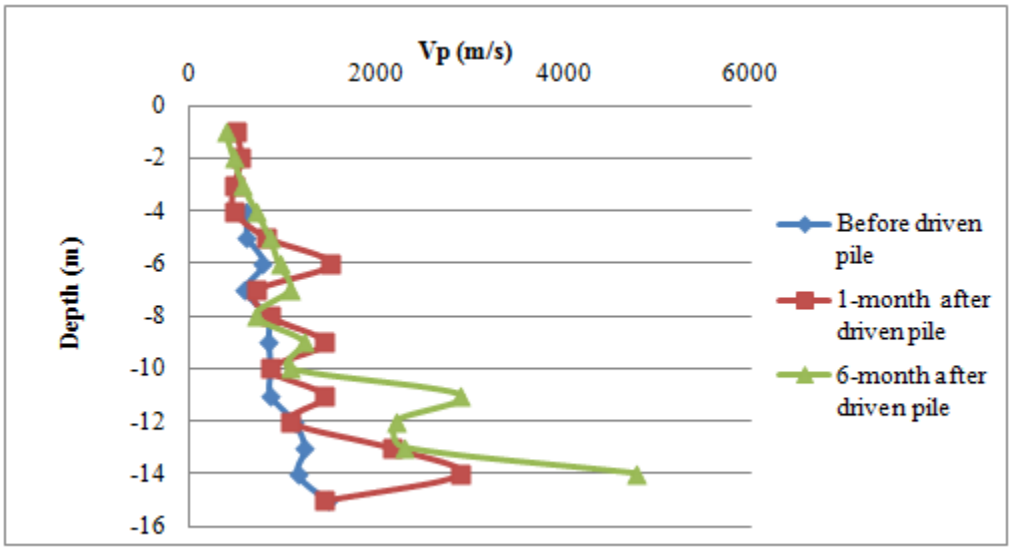

(b) Profile S2

Figure (6). Relationship between compression wave velocity versus depth for ProfilesS1 and S2 before driven piles and after (1-6) month.

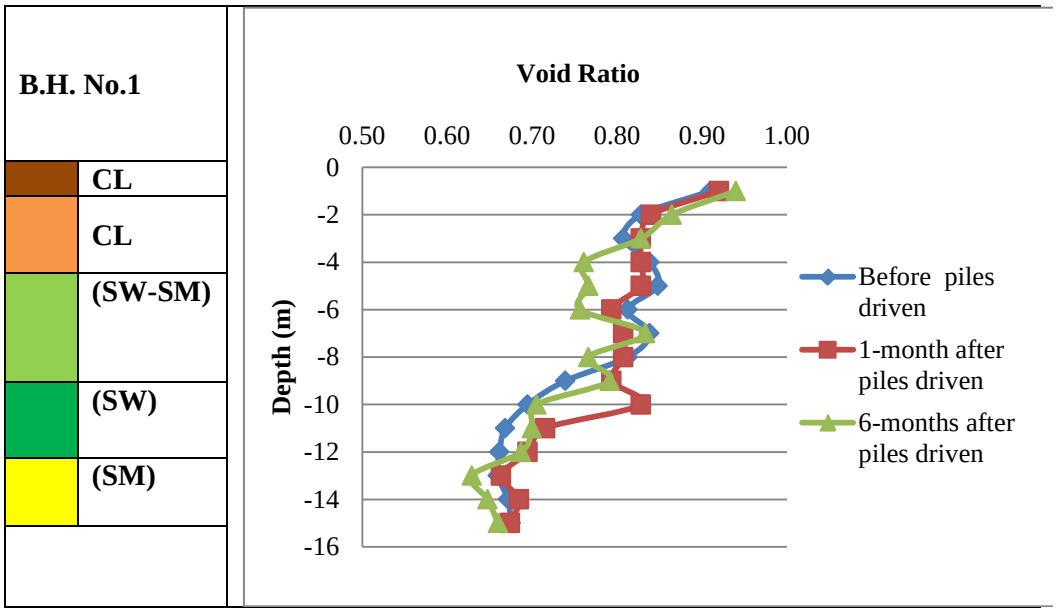

(a) Profile S1

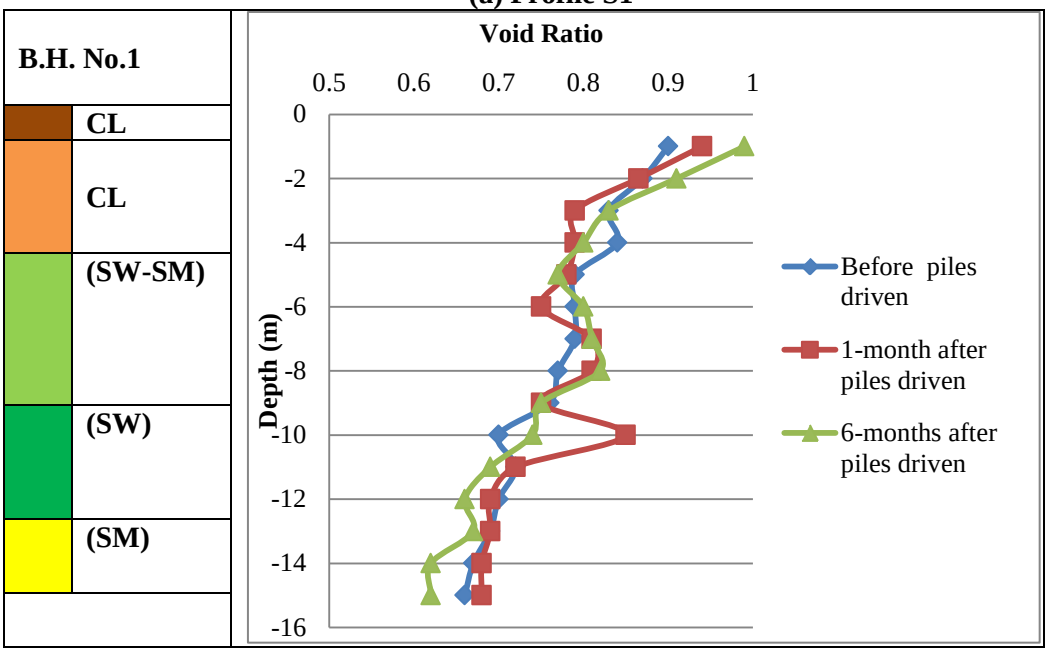

(b) Profile S2

Figure (7). Void ratio with depth for Profile S1 and S2 before and after piles driven.

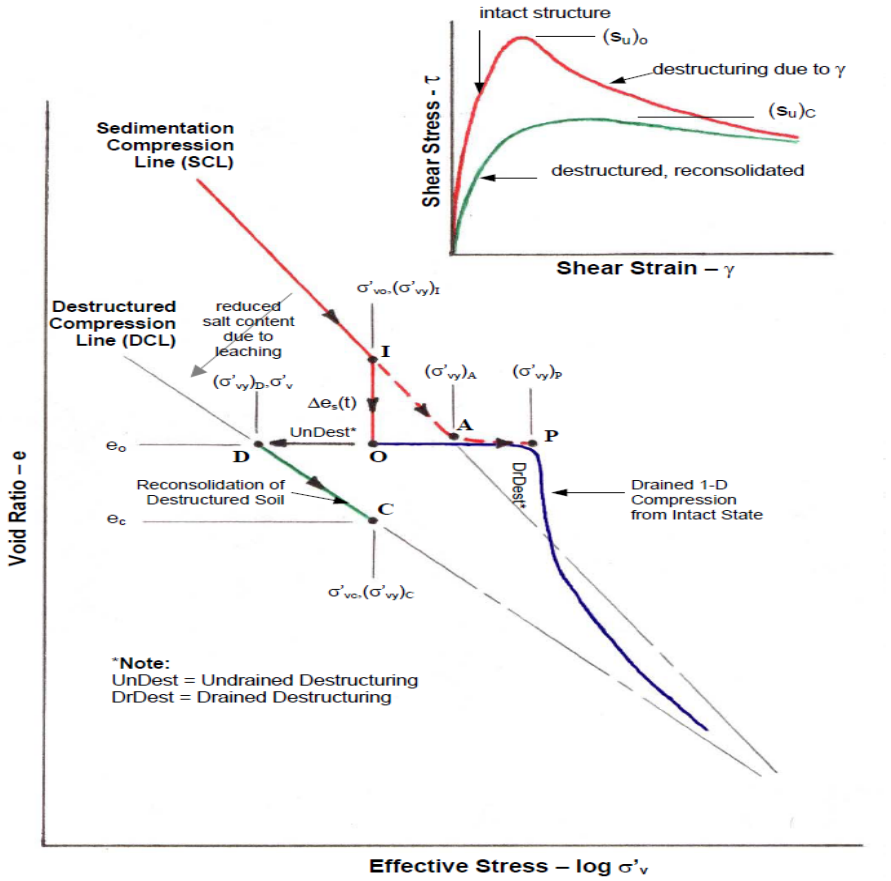

Figure (8). Development of micro-structure and behavior of structured and destructured soils in one-dimensional consolidation and undrained shear strength [13].

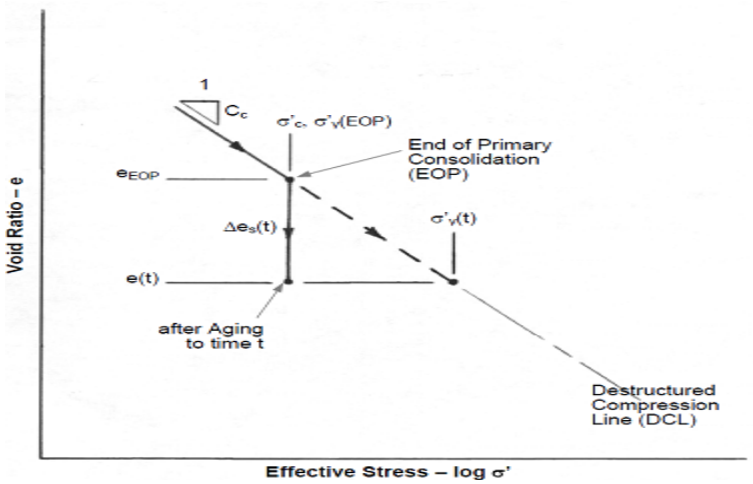

Figure (9). Changes in yield stress due to aging [13].

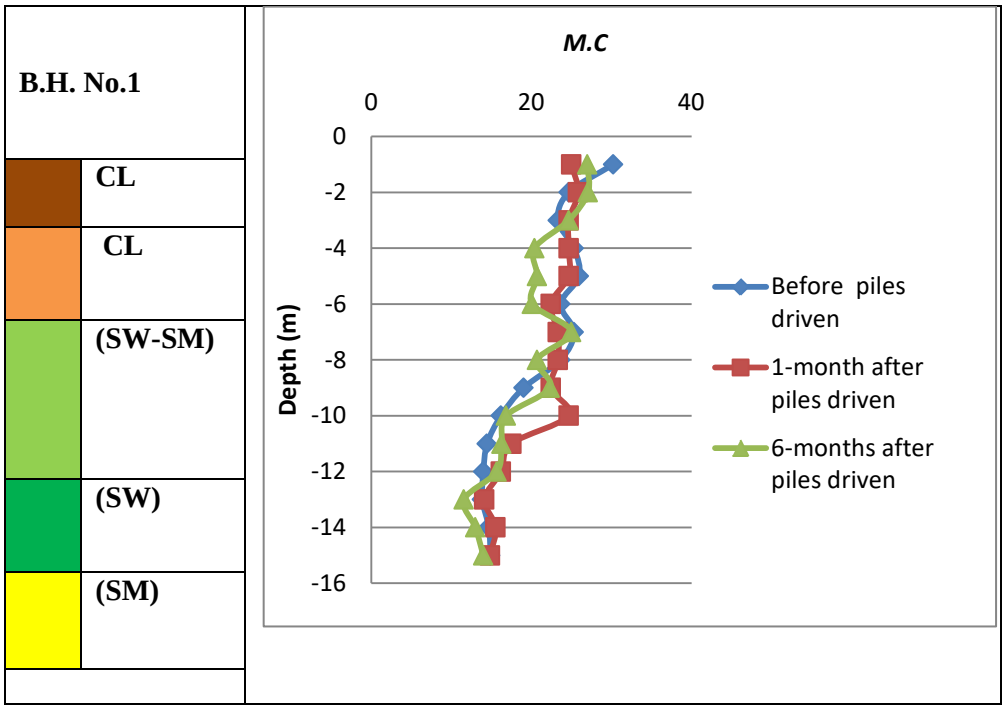

(a) Profile S1

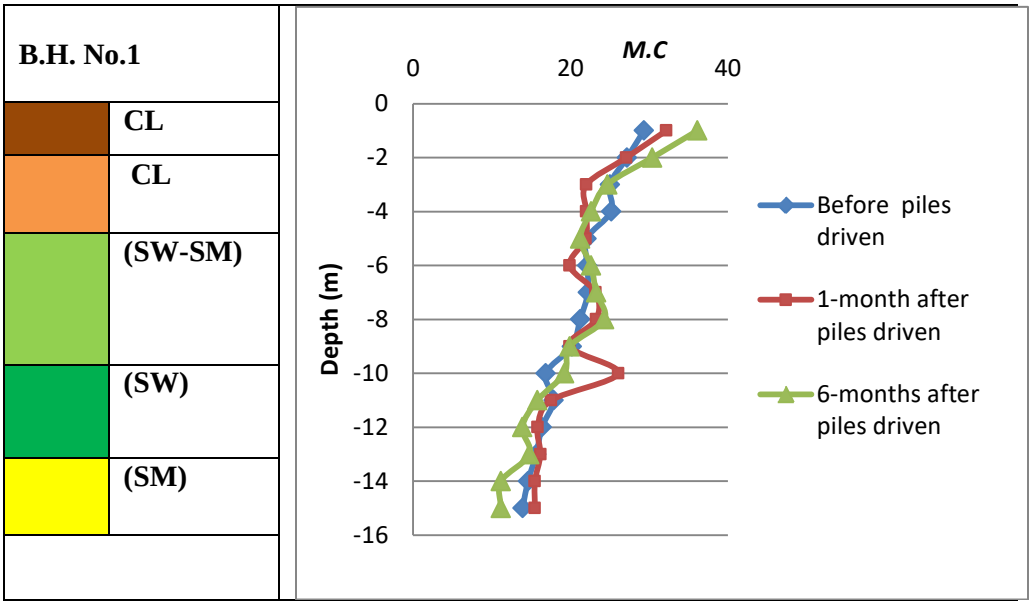

(b) Profile S2

Figure (10). Moisture content with depth for Profile S1and S2 before and after piles driven.

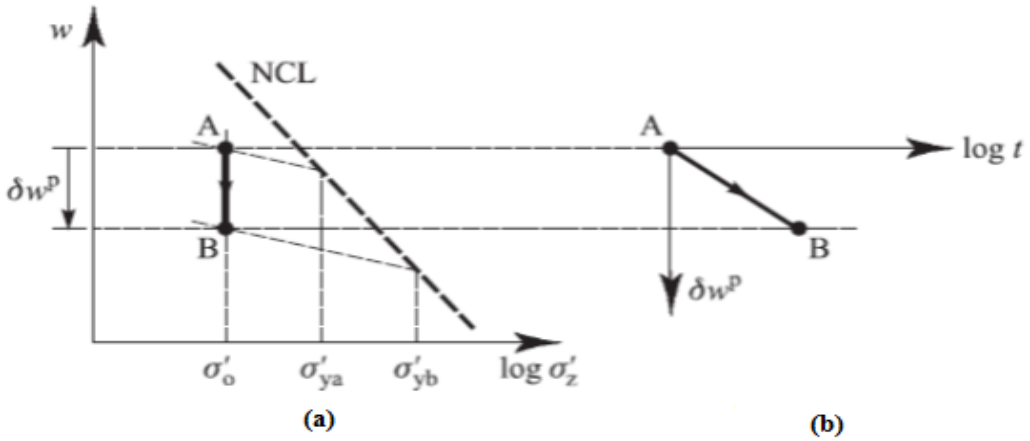

Figure (11). Change of yield stress ratio due to creep of fine grained soil [14].

CONCLUSIONS

The main conclusions drawn from this study are:

1.There is direct relation between the increase in soil undrained shear strength with yield stress ratio and reverse relation with moisture water content and void ratio.

2.The increase in undrained shear strength and yield stress ratio are observed in the clay soil layer at 3-5 m in depth with low moisture content and void ratio due to aging factor. While at depth of 1-3 m, the reverse was noticed due to shear force from driven pile leading to increase the moisture water content and void ratio.

3.Immediately after pile installation, the undrained shear strength of the soil next to the pile has been significantly reduced below the intact strength of the material.

4.As the excess pore pressures dissipate and the effective stresses increase, the soil next to the pile consolidates to a lower void ratio than in its natural state. The undrained shear strength increases according to the $(S_u/\bar{\sigma}_V)$ ratio of the soil in its partly to completely destructured state.

5.Upon completion of the pore pressure dissipation process, the undrained strength of the soil next to the pile will have reached a value which depends on the magnitude of the principal effective stresses around the pile, and on the $S_u/\bar{\sigma}$ ratio of the partly to completely destructured soil.

6.The shear strength may continue to increase with time after completion of dissipation of excess pore water pressure due to aging processes.

7.The results have provided good overall views of the shear strength increases and their distributions and the estimated values are also of the right sizes.

REFERENC

[1]. Hasan, A.M., "Evaluating geotechnical properties from geophysical data", M. Sc. Thesis, Building & Construction Engineering Dept., University of Technology, 115 P, 2006.

[2]. Khalil, M.H. and Hanafy, S.M., "engineering applications of seismic refraction method: A field example at Wadi Wardan, Norteast Gulf of Suez, Sinai, Egypt", J. of Applied Geophysics, Vol. 65, pp. 132-141,2008.

[3]. Shakir, A.M., "Geophysical and geotechnical study of a proposed tunnel site at Al-Najaf City, Southern Iraq", Ph.D Thesis, University of Baghdad, 2012.

[4]. Ozcep,F., Guzel,M., Kepekci,D., Laman,M., Bozdag,S., Cetin,H. and Akat,A., "Geotechnical and geophysical studies for wind energy systems in earthquake-prone areas: Bahce (Osmaniye, Turkey) case", Int. J. of the Physical Sciences, Vol. 4, No. 10, pp. 555-561, 2009.

[5]. Korkmaz,B. and Ozcep,F., "Fast and efficient of geophysical and geotechnical data in urban microzonation studies at small scales: Using Sisli/ Istanbul (Turkey) as example", Int. J. of the Physical Sciences, Vol. 5, No. 2, pp. 158-169, 561, 2010.

[6]. Larson, R. and Mattsson, H., "Settlement and shear strength increase below embankments", Linkoping, Swedish Geotechnical Institute (SGI), Report No. 63, 2003.

[7]. Kearey P, Brooks M, Hill I, "An introduction to geophysical exploration", Blackwell Science, Oxford, 2002.

[8]. Zhao, Y., "In situ soil testing for foundation performance prediction", Ph.D Thesis. Magdalene College. University of Cambridge, 2008.

[9]. Komurka, V.E., Wagner, A.B. and Edil T. B., "Estimating soil/pile set-up", Wisconsin Highway Research Program, No. 0092-00-14, Wagner Komurka Geotechnical Group, Inc., and the Department of Civil & Environmental Engineering, University of Wisconsin-Madison, 2003.

[10]. Simulia, "Analysis of driven pile setup with abaqus/standard", Abaqus Technology Brief. Tb- 06-pile-1, 2007.

[11]. Ladd, C.C. and Foott, R. "New design procedure for stability of soft clays", ASCE, Journal of the Geotechnical Engineering Division, Vol. 100, No. GT 17, pp. 763-786, 1974.

[12]. Bjerrum, L., "Engineeing geology of normally consolidated marine clays as related to settlements of building", Geotechnique, Vol. 17, No.2, pp. 83-119, 1967.

[13]. Weech, C. N., "Installation and load testing of helical piles in a sensitive fine-grained soil", M.Sc. Thesis, The University of British Columbia, 2002.

[14]. Atkinson, J. H., "The Mechanics of Soil and Foundations". Second Edition, Taylor and Francis Group, 475P, 2007.